

Structure of duplex CrN/NbN coatings and their performance against corrosion and wear

SAVISALO, T., LEWIS, D. B., LUO, Q. <<http://orcid.org/0000-0003-4102-2129>>, BOLTON, M. and HOVSEPIAN, P. E. <<http://orcid.org/0000-0002-1047-0407>>

Available from Sheffield Hallam University Research Archive (SHURA) at:

<http://shura.shu.ac.uk/1148/>

This document is the author deposited version. You are advised to consult the publisher's version if you wish to cite from it.

Published version

SAVISALO, T., LEWIS, D. B., LUO, Q., BOLTON, M. and HOVSEPIAN, P. E. (2007). Structure of duplex CrN/NbN coatings and their performance against corrosion and wear. *Surface and Coatings Technology*, 202 (9), 1661-1667.

Copyright and re-use policy

See <http://shura.shu.ac.uk/information.html>

Structure of duplex CrN/NbN coatings and their performance against corrosion and wear

T. Savisalo^{a,□}, D.B. Lewis^a, Q. Luo^a, M. Bolton^b, P. Hovsepian^a

^a Sheffield Hallam University, Materials Research Institute, Howard St, S1 1WB, Sheffield, United Kingdom.

^b Eltro (GB) Ltd. Unit B4 Armstrong Mall, Southwood Business Park, Farnborough, Hampshire, GU14 0NR, United Kingdom.

Abstract: In tribological applications the coating-substrate combination can be considered as a system, since both greatly influence the properties of that affect the tribological performance. Further, it is often desirable that both high wear resistance and corrosion resistance can be achieved even when low cost and easily machineable substrate materials are considered. Duplex surface treatment combining pulse plasma nitriding and PVD coating can provide solution for excellent wear and corrosion resistance for low alloy and constructional steels.

In this work three different pulse plasma nitriding processes were carried out prior to the CrN/NbN PVD coating to attain high surface hardness and enhanced load bearing behaviour for S154 high strength construction steel. The phase composition of the compound layer, formed in the nitriding process, was found to greatly affect the tribological properties of the duplex system. The compound layer with high amount of ϵ -phase contributed to superior corrosion and wear resistance, whereas the ductile γ' -phase compound layer provided better impact resistance and enhanced. The best duplex treated S154 samples had wear resistance comparable to that of similarly coated HSS. The corrosion resistance was also improved by duplex process. If anodic current at +500 mV vs. SCE is considered as criteria, the best system has almost 3 orders of magnitude lower corrosion current than with the PVD coating alone.

Key Words: Duplex; PVD; CrN/NbN; Nitriding; Corrosion; Wear

1. INTRODUCTION

PVD coatings have been shown to be very valuable in surface engineering providing a variety of desirable surface properties such as appearance, high wear resistance, low friction and good corrosion resistance [1,2]. In tribological applications coating substrate combination should be considered as a composite since both greatly affect physical properties of the system. Very low wear rates have been reported with coated hard steels such as high speed steel [1,3,4] as these highly stressed hard coatings need strong support. If the load bearing capacity of the substrate is exceeded the wear is greatly increased [5,6]. Further, good corrosion resistance has been achieved with coated stainless steels [7–9]. In tribological applications both of these properties should be achieved simultaneously in combination with low price and easily machineable substrate material. Ductility of the substrate may also be required as components are commonly required to withstand impacts and deformation.

Nitriding is a commonly used surface treatment method to improve surface hardness and wear resistance of steels. The relatively inert white layer can also provide improved corrosion performance [10]. Lately nitriding has been used in combination with PVD coatings (duplex coatings) with promising results [5,10–16]. Nitriding process can be done prior to PVD process with any conventional method or in conjunction with PVD process with low pressure plasma nitriding. Nitriding provides increased surface hardness of HV=1000+ providing the support that is required by the coating as well as reducing the stress gradients at the interfaces with the PVD coating (HV=3500+). The compound layer (Fe₄N or Fe₃N) has been regarded to be detrimental to adhesion and thus avoided or removed mechanically [10,14], yet it has been shown in some instances to improve wear resistance [5,11,17].

CrN/NbN superlattice coatings have been developed to withstand wear and corrosion. These coatings show good corrosion and wear resistance even in very aggressive conditions [1,4]. Metal ion pre-treatment in ABS (Arc Bond Sputtering) process has been shown to enhance adhesion and corrosion resistance further. Cr ion etching has been shown to provide optimal adhesion while Nb ions may be used for enhanced corrosion performance [3,4,8,18,19].

In this paper novel duplex nitriding-PVD CrN/NbN superlattice system is introduced and characterised. Microstructural analysis are presented and their effects to mechanical and corrosion properties discussed.

2. Experimental

The coatings were deposited on ground and polished (Ra=0.05 µm) S154 steel and High Speed Steel (HSS) disks with 30 mm diameter. S154 is low alloy, high strength construction steel, with good machineability and weldability (composition: C 0.35, Si 0.3, Mn 0.6, Cr 0.7, Mo 0.6, Ni 2.5, similar to AISI 4340). The HSS samples were used as a reference and were not nitrided. The nitriding was done in a commercial lowpressure pulse plasma nitriding process by Eltro Ltd., UK. Three different nitriding parameter sets were used. The atmosphere during the process was 3:1 hydrogen/nitrogen gas mixture. Sample 1 was nitrided for 6 h in 520 °C

(process 1), sample 2 for 3 h in 480 °C continuing further with 14 h in 520 °C (process 2), and sample 3 for 40 h in 530 °C (process 3). The main advantage of pulsed plasma process vs. plasma nitriding is improved process control through minimised arcing and more uniform heat distribution. Prior to coating a porous surface layer was removed with light mechanical polishing after which the samples were cleaned on an automated cleaning line comprised of a series of ten ultrasonically agitated cleaning and rinsing baths and a vacuum drier.

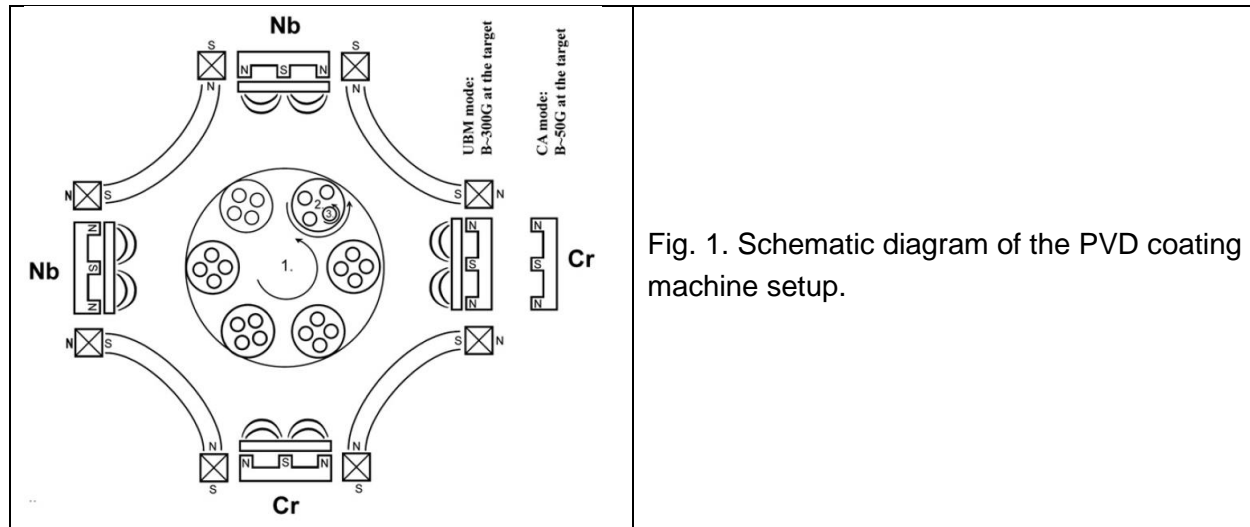


Fig. 1. Schematic diagram of the PVD coating machine setup.

The coatings were deposited at 450 °C using industrial sized multi-target HTC 1000-4 ABS combined cathodic arc/unbalanced magnetron sputtering (UBM) coating system, manufactured by Hauzer Techno Coatings BV. The coater is a four cathode drum type batch coating machine with the cathodes arranged in a closed field configuration. The coatings were done using configuration with two niobium and two chromium targets arranged as shown in Fig. 1. The samples were subjected to 3 fold rotation in X–Y plane during deposition, which ensures uniform coating thickness even for three dimensional parts. The process consisted of the following steps: heating and target cleaning, cathodic arc Cr ion etching using high bias voltage, UBM deposited CrN base layer and UBM deposited CrN/NbN nanostructured layer with lattice period of about 3 nm. The parameters used during the coating deposition are presented in more detail in Table 1. The properties and the structure of the coating have been studied in detail by Hovsepian et al. [8,20].

2.1. Coating characterization

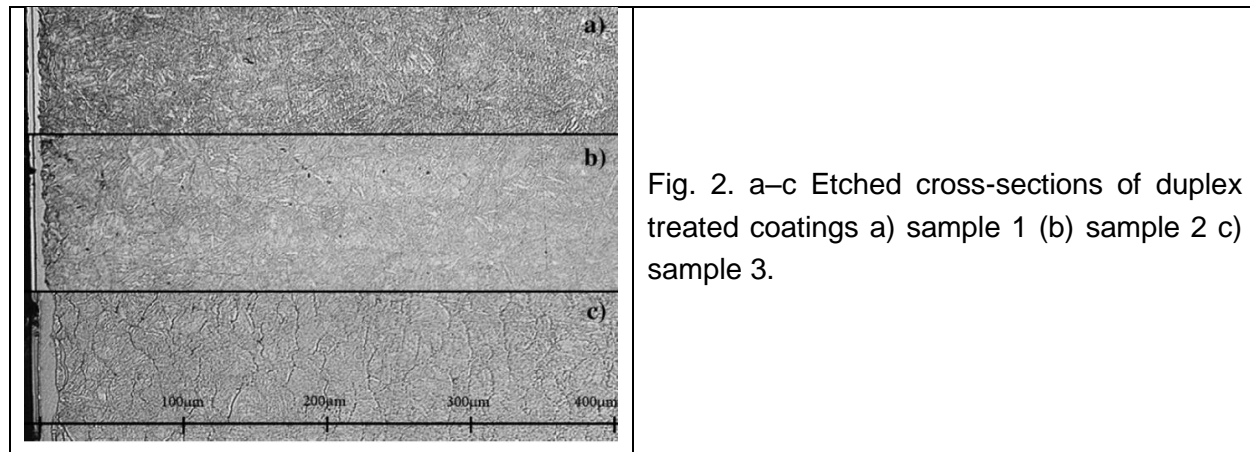
The mechanical properties of the samples were characterized using a series of analytical techniques. CSEM Revetest was used to measure adhesion (critical load, L_c), Mitutoyo MVK-G1 for the hardness measurements of the coating (H_k , 25 g normal load) and CSEM pin-on-disk tribometer for measuring the sliding wear rate. For the sliding wear test Al_2O_3 ball was used at 5 N load and 10 cm/s linear speed. The wear was measured after 60 k laps. Impact tests were performed using a CemeCon impact tester using 350 N load with Ø6 mm 100Cr6 ball. Hardness-

Table 1 Coating deposition parameters

Nitriding process (3:1 hydrogen/ nitrogen atmosphere)	Sample 1 (170 μm case depth)6 h @ 520 °C Sample 2 (290 μm case depth)3 h @ 480 °C followed by 14 h @ 520 °C Sample 3 (400 μm case depth)40 h @ 530 °C
Polishing & cleaning	
Pump-down and heating:	400 °C with pressure $<7 \times 10^{-5}$ mbar
Cr ⁺ etching(20 min)	Arc current: $I=100\text{A}$, Bias voltage: $U_b=-1200\text{ V}$ Pressure: $p=1 \times 10^{-3}$ mbar
CrN(30 min)	Power: 2 Cr targets with 5 kW Bias voltage: $U_b=-75\text{ V}$ Pressure: $p=3.8 \times 10^{-3}$ mbar
CrN/NbN(150 min)	Power: 2 Cr targets with 5kW and 2 Nb targets with 10 kW Bias voltage: $U_b=-120\text{ V}$ Pressure: $p=3.6 \times 10^{-3}$ mbar Cr: 2 * 5 kW, Nb: 2 * 10 kW

depth profiles of the nitrided samples were generated from a polished cross-sections using Mitutoyo MVKG1 hardness tester with Vickers diamond tip (Hv,25 g normal load).

Potentiodynamic polarisation measurements were performed in 3% NaCl solution using a 3-electrode cell with a Saturated Calomel Reference Electrode (SCE) using on ACM Gill AC potentiost at over a potential range of ± 1000 mV vs. SCE at scan rate of 0.5 mV/s. Prior to polarisation measurements samples were cleaned cathodically at -1.5 V for 100 s and then allowed to equilibrate at Open Circuit Potential (OPC) for 40 min. Microstructure was analysed using XRD (Philips PW1820). Glancing angle (1°) and Bragg-Brentano scans were performed prior coating deposition to characterise the top layer of nitrided substrates. Cross sections and the impact craters were investigated using optical microscope and Philips XL40 SEM.



3. Results

The polished and etched cross sections of the coatings can be seen in the Fig. 2. The nitriding case depths were determined to be 170 μm , 290 μm and 400 μm with samples 1, 2 and 3 respectively. The coating thickness was about 4 μm consisting of $\sim 0.5\text{ }\mu\text{m}$ CrN base layer and

about 3.5 μm CrN/NbN superlattice. The hardness of the coating was roughly constant with all samples, $\text{HK}_{25\text{g}}=3000$. The compound layer is also visible in the images with thickness varying from $\sim 5\text{ }\mu\text{m}$ with sample 1 (170 μm) to $\sim 15\text{ }\mu\text{m}$ with sample 3 (400 μm). The nitriding effect can be seen up to a depth of 500 μm with sample 3. The cross section micrographs showed no instability of the compound layer during the coating process (ie. black layer).

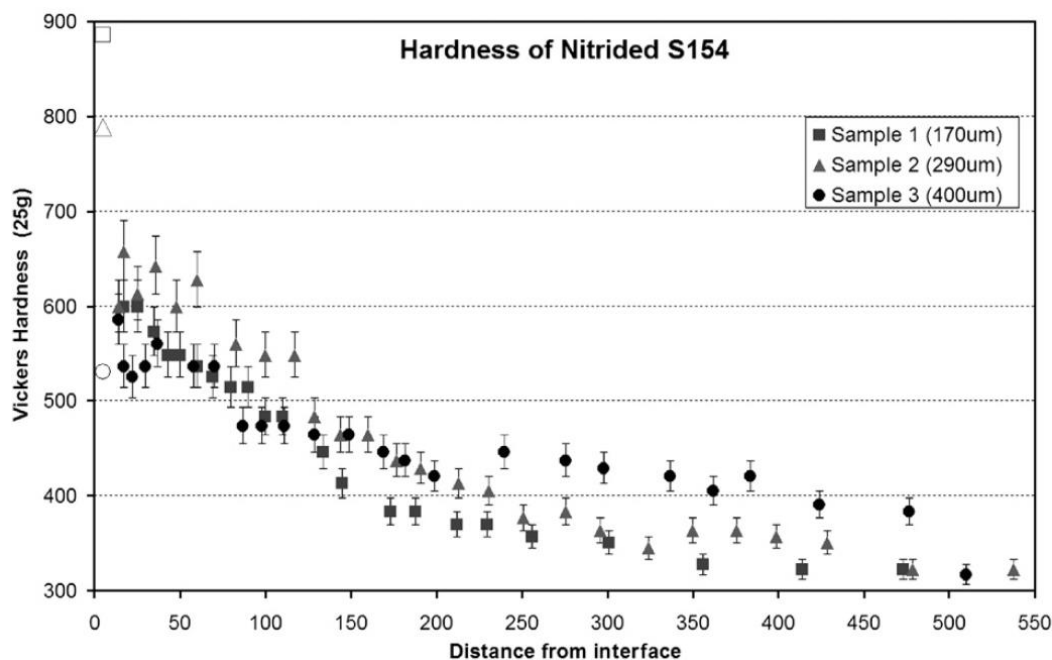


Fig. 3. Hardness-depth profile of the nitrided S154 steel samples.

Hardness-depth profile ($\text{Hv}_{25\text{g}}$) of the nitrided zone can be seen in Fig. 3. The open markers indicate the measurements done from the surface, while the others are from the cross section. The highest surface hardness was measured with sample 1 ($\text{Hv}_{25\text{g}}=890$), samples 2 and 3 being somewhat softer at $\text{Hv}_{25\text{g}}=790$ and $\text{Hv}_{25\text{g}}=530$, respectively. All of these are notably higher than bulk hardness of $\text{HV}=320$. After the compound layer (10 μm) up to the depth of about 200 μm the highest hardness was measured from sample 2. The hardness 100 μm below the surface was measured to be from 480 (Sample 3) to 540 (Sample 2). Sample 3 has the hardness of $\text{Hv}_{25\text{g}}=400+$ up to the depth of 400 μm while the samples 1 and 2 retain the same hardness to the depths of 160 μm and 240 μm respectively.

The micrographs of the impact craters after 1 million impacts can be seen in Fig. 4. Sample 1 has the largest impact crater with diameter of 495 μm . The coating is fully intact yet there are number of circular cracks clearly visible near the edge of the crater. The diameter of the impact crater of sample 2 was measured to be 475 μm . It also has some visible cracks around the edge of the crater yet not to the same extent as sample 1. The sample 3 showed excellent impact resistance with the smallest impact crater ($d=460\text{ }\mu\text{m}$) and shows no sign of cracks or delamination. The results can be explained by the previous results of microstructure and hardness measurements as the ductile γ' phase compound layer can deform under high

pressure while the brittle ϵ phase fractures. The higher case depth on the other hand provides better support for these high loads as indicated by the crater size.

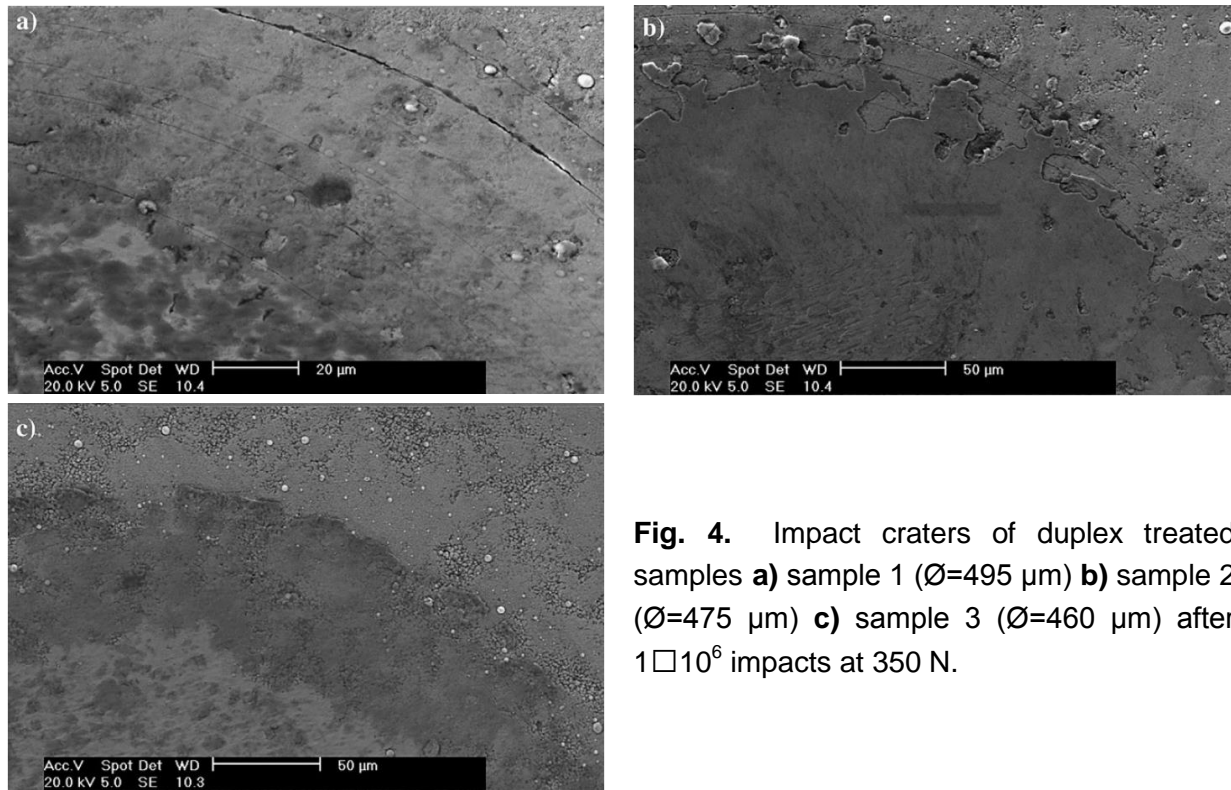


Fig. 4. Impact craters of duplex treated samples **a)** sample 1 ($\varnothing=495 \mu\text{m}$) **b)** sample 2 ($\varnothing=475 \mu\text{m}$) **c)** sample 3 ($\varnothing=460 \mu\text{m}$) after 1×10^6 impacts at 350 N.

Sample 3 also had the highest critical load values in scratch test ($L_c=60 \text{ N}$). Sample 2 had critical load of 45 N and sample 1 had 35 N. The coated HSS sample had critical load of 45 N, while the coating on the un-nitrided S154 showed failures at a normal load of mere 20 N. The Fig. 5 shows SEM image and EDS map of a typical failure on the samples 1 and 2 with brittle type fracture going through compound layer and the coating.

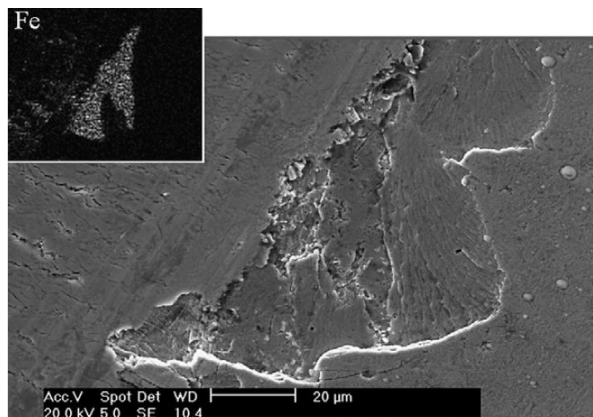


Fig. 5. SEM image of coating adhesion failure on sample 1 with EDS map of Fe.

The calculated sliding wear coefficients of the coated samples, along with nitrided S154 steel without the PVD coating and HSS (not nitrided) with the same PVD coating can be seen in Fig. 6. Sample 1 has clearly the smallest sliding wear rate ($2.6 \times 10^{-15} \text{ m}^2/\text{N}$), which is similar to the HSS sample with significantly higher hardness ($H_v=820$). Samples 2 and 3 had slightly

higher wear rates (6.7 and $10.7 \times 10^{-15} \text{ m}^2/\text{N}$ respectively). All the duplex treated samples had significantly lower wear than the reference samples of each individual process. The high wear rate of the

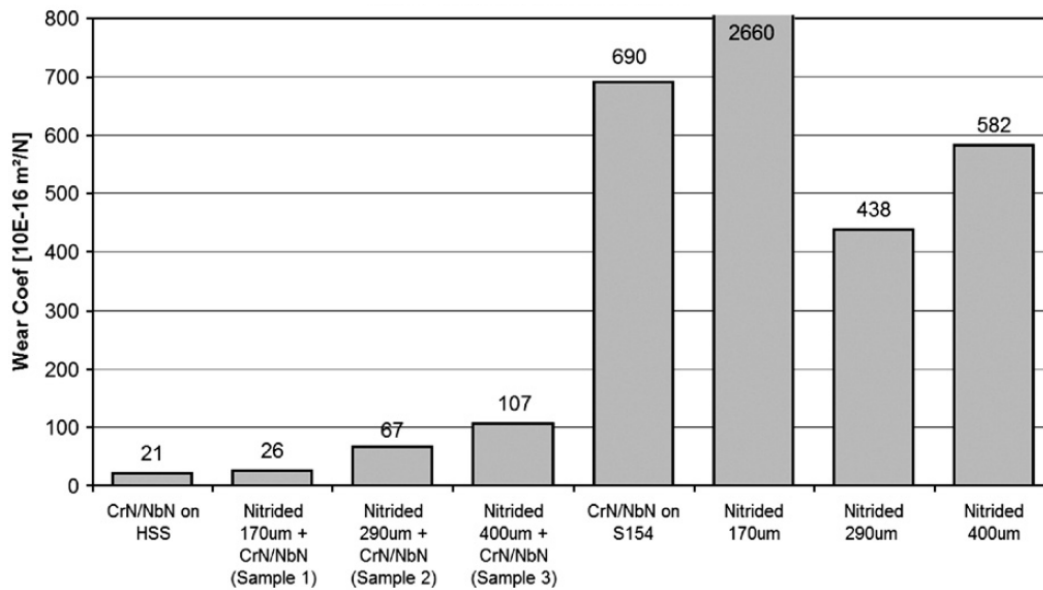


Fig. 6. Sliding wear coefficients of S154 with different surface treatments.

CrN/NbN coated sample ($6.9 \times 10^{-13} \text{ m}^2/\text{N}$) shows how poorly the hard, wear resistant coatings perform when the load bearing capacity of the substrate is exceeded. The wear rate was two orders of magnitude higher than the duplex treated samples and one order of magnitude higher than electrodeposited hard chrome ($5.8 \times 10^{-14} \text{ m}^2/\text{N}$) [20]. The wear of the nitrided samples (without the CrN/NbN PVD coating) was high ranging from $4.4 \times 10^{-13} \text{ m}^2/\text{N}$ (Sample 2) to $2.7 \times 10^{-12} \text{ m}^2/\text{N}$ (Sample 1).

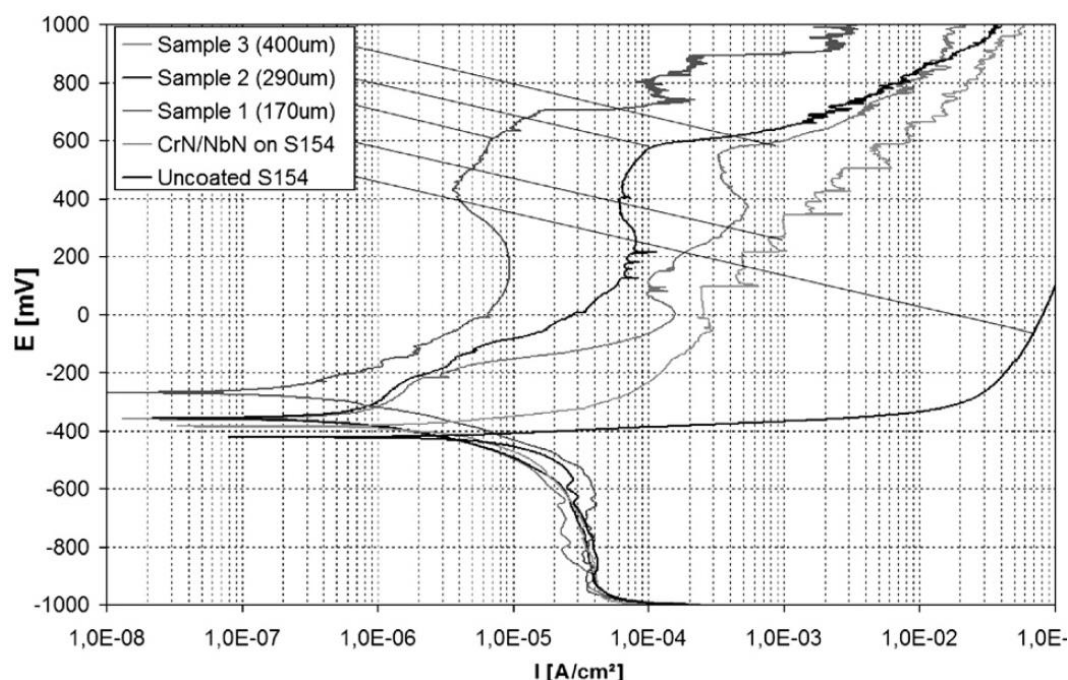


Fig. 7. Results of potentiodynamic polarisation tests of treated and untreated S154 steel in 3% NaCl solution.

The results of the potentiodynamic polarisation tests can be found in Fig. 7. Comparing the duplex treated samples to the reference samples shows that significant improvement is achieved with duplex approach. The untreated substrate performed the worst with no passivation in the 3% NaCl solution. The PVD coated S154 sample (no nitriding) exhibited some “passive like” behaviour with anodic current densities around 3 orders of magnitude less than the untreated reference. All duplex treated coating outperformed the PVD coated reference. Comparing different duplex treated samples, the sample 1 has the highest corrosion resistance followed by sample 2 and 3 respectively. If anodic current at +500 mV vs. SCE is considered as criteria, the best system (sample 1) has almost 3 orders of magnitude lower corrosion current than un-nitrided sample. The corrosion damage on these samples is localised, with size of the pits increasing in diameter and depth from sample 1 to sample 3 (see Fig. 8). No delamination of the coating was observed near the pit locations.

The XRD patterns of the samples before coating can be seen in Fig. 9. Samples 1 and 2 have very similar spectra showing two ferrous nitride phases, γ' (gamma prime, Fe_4N) and ϵ (Fe_3N) while sample 3 is virtually fully γ' phase. The glancing angle measurement show higher

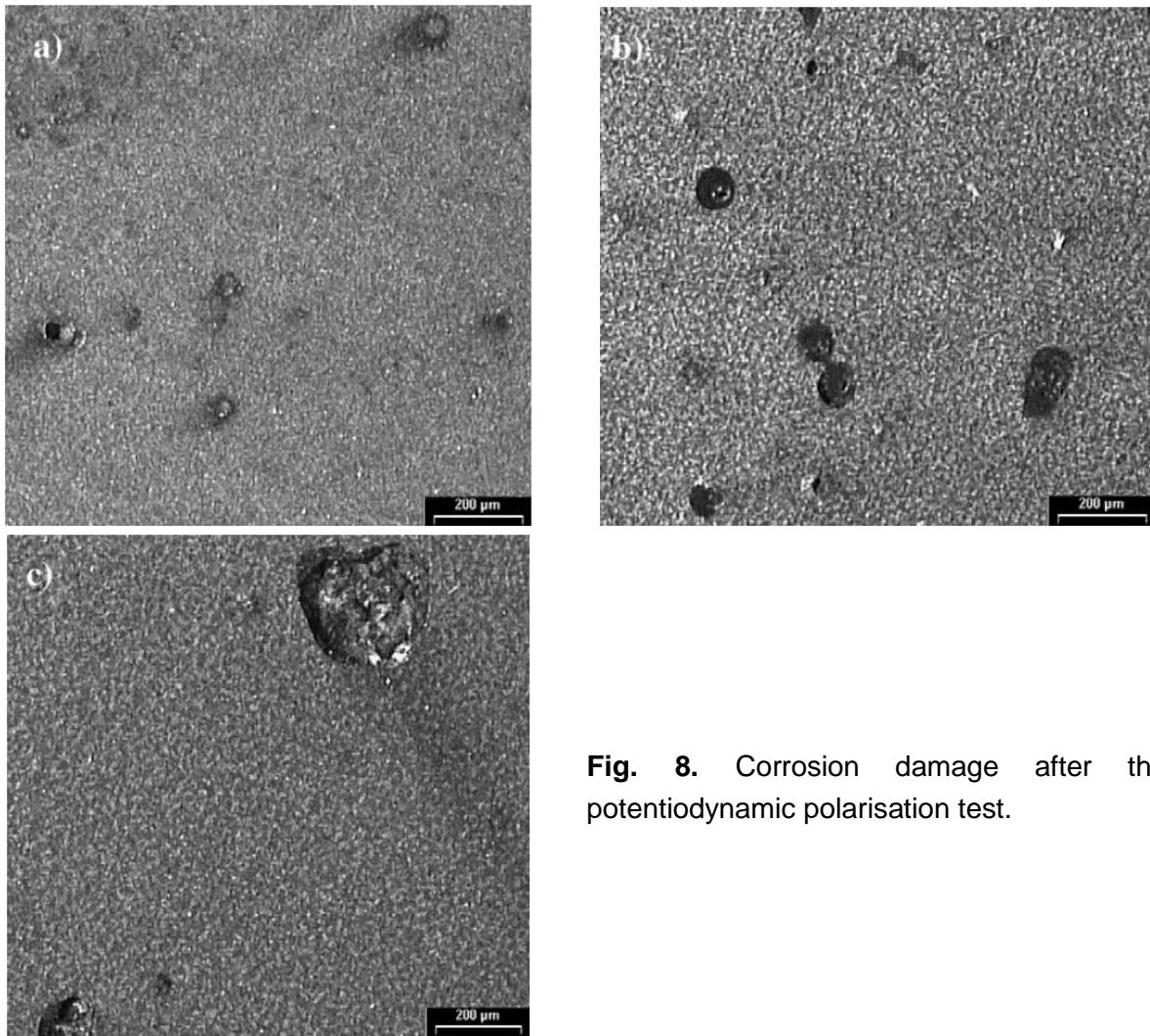


Fig. 8. Corrosion damage after the potentiodynamic polarisation test.

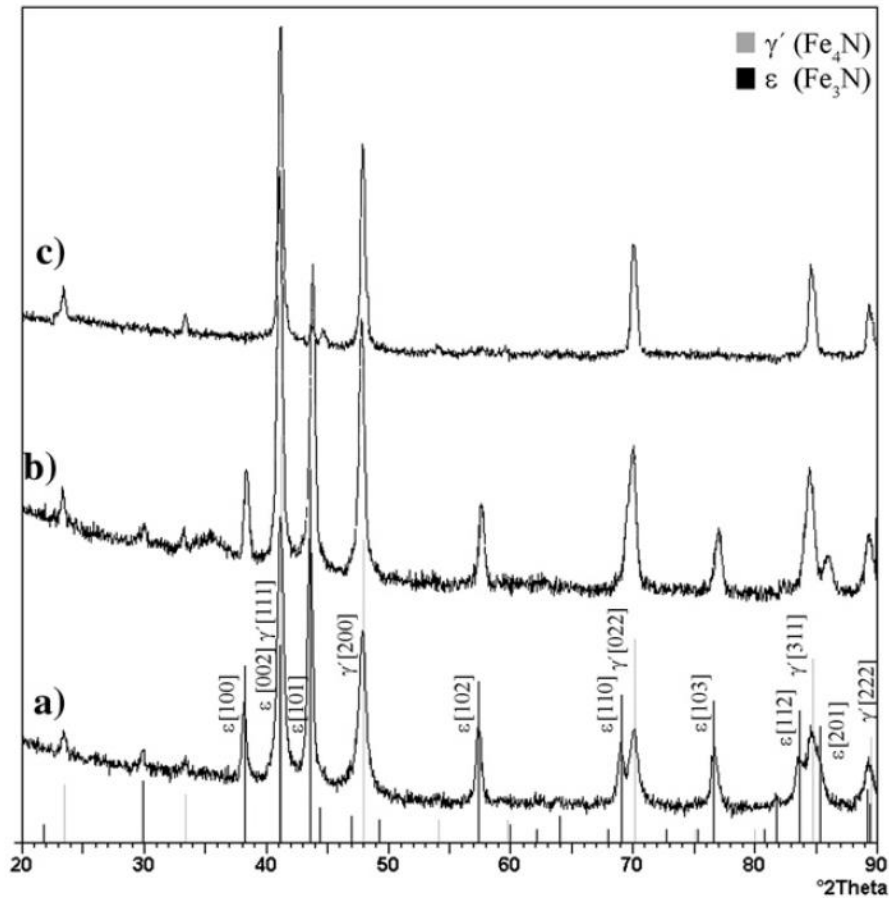


Fig. 9. 1° glancing angle XRD scans of the nitrided substrates prior PVD coating.

proportion of ϵ phase with all samples than the Bragg–Bretano measurements, indicating that there is more ϵ phase at surface regions. The apparent phase composition can be seen in Table 2 along with the summary of the mechanical properties of the samples.

Table 2 Summary of properties

	CrN/NbN on S154	Duplex treated S154		
		sample 1 (170 μm)	sample 2 (290 μm)	sample 3 (400 μm)
Compound layer 1° GA	N/A	4 μm , 48% ϵ phase	7 μm , 42% ϵ phase	10 μm , 12% ϵ phase
Compound layer 1° B–B		32% ϵ phase	23% ϵ phase	7% ϵ phase
Surface hardness	$\text{HV}_{25\text{g}}=320$	$\text{HV}_{25\text{g}}=890$	$\text{HV}_{25\text{g}}=790$	$\text{HV}_{25\text{g}}=530$
Sliding wear rate	$6.9 \times 10^{-14} \text{ m}^2/\text{N}$	$2.6 \times 10^{-15} \text{ m}^2/\text{N}$	$6.7 \times 10^{-15} \text{ m}^2/\text{N}$	$1.1 \times 10^{-14} \text{ m}^2/\text{N}$
Adhesion (L_c)	25 N	35 N	45 N	60 N
Impact resistance		Fair	Fair	Good
Impact crater		495 μm	475 μm	460 μm
Anodic corrosion current density at +500 mV vs. SCE	$2.6 \times 10^{-3} \text{ A/cm}^2$	$5.0 \times 10^{-6} \text{ A/cm}^2$	$7.3 \times 10^{-5} \text{ A/cm}^2$	$3.5 \times 10^{-4} \text{ A/cm}^2$

4. Discussion

The nitriding process and the compound layer microstructure can be seen to greatly affect the mechanical and chemical properties of the duplex treated (nitriding+PVD coating) S154 steel. The compound layer is generally thought to lead to adhesion failure of the PVD coating due to porous top layer and instability at high temperatures (500 °C). It can however be beneficial due to its high hardness and improved corrosion resistance [21]. G. Nayal et al. demonstrated that metal ion etching prior to PVD coating may be required to achieve acceptable adhesion on the compound layer [17]. The duplex treated S154 investigated in this work exhibited excellent adhesion and tribological performance.

The micrographs and the hardness measurements show that the microstructure of the compound layer changes with nitriding process. The two common phases γ' (Fe₄N, FCC) and ϵ (Fe₃N, Hexagonal) were detected in the compound layer. The γ' phase is generally regarded as softer, more impact resistant phase and ϵ phase as hard and brittle. In tribological applications ϵ phase is generally preferred. [10] The apparent phase composition of the compound layers showed that samples 1 and 2 have roughly 50% of the hard and corrosion resistant ϵ phase (48% and 42%, respectively), while sample 3 is mostly gamma prime phase (88% γ' phase). The 1° glancing angle measurement show higher proportion of ϵ phase with all samples than the Bragg- Bretano measurements (32%, 23% and 7%), indicating that there is more ϵ phase at surface regions. This correlates well with the surface hardness measurements as ϵ phase is known to be hard and brittle and γ' phase softer and more ductile.

The surface hardness of the nitrided substrate correlates well with the pin-on-disk wear behaviour. The wear rate of the sample 1 (170 μm) is roughly equal to the wear rate of the same coating on M2 High Speed Steel, the latter having almost 3 times the bulk hardness of S154 steel. The wear rates of all duplex coatings prepared are remarkably low. All duplex treated samples clearly out-performed nitrided samples and the PVD coated S154 with no nitriding treatment. The poor performance of the PVD coating on untreated S154 steel is thought to be caused by insufficient support to the coating under the 5 N normal load subjected to the alumina ball leading to crack propagation through the coating causing accelerated wear.

There were considerable differences in the fatigue and wear behaviour between the different samples. Though the Sample 3 did not perform very well in the wear test it exhibited excellent impact resistance. The longer nitriding process used for Sample 3 yielded largest case depth and the thickest compound layer ($\sim 15 \mu\text{m}$). This combination gives good support to the coating as shown by the impact crater with the smallest in diameter and absolutely no sign of cracks or delamination. Sample 3 also had the highest critical load in the scratch test exceeding the HSS by 15 N (60 N vs. 45 N). The excellent adhesion is attributed partially to the ductile nature of the γ' rich compound layer and the gradual reduction of the hardness that reduces the stress concentration at the interface as the diamond tip of the scratch tester deforms the surface. The crystal structure of the compound layer (γ' phase, FCC) is also same as with the coating (FCC), which may introduce local epitaxial growth enhancing the adhesion.

Despite the excellent wear behaviour sample 1 failed at relatively low critical load value in the adhesion test. We expect that to be caused by a brittle fracture initiating within the compound layer rather than simple delamination of the coating. Both of the coatings with the ϵ phase (samples 1 and 2) also showed cracks in the impact crater further showing the brittle nature of the ϵ phase compound layer. Brittle behaviour was confirmed by SEM observation of the scratch scar (Fig. 5).

The duplex treatment has significant positive impact to the corrosion resistance of the S154.

All coated samples showed “passive like” anodic behaviour. Since the corrosion is localised at the defect locations and the coating remain passive the anodic current density can be related to the active substrate area. At an anodic potential of +500 mV vs. SCE sample 1 has almost 3 orders of magnitude smaller corrosion current density than the same coating without nitriding and 2 orders of magnitude lower than sample 3. This indicates that the ϵ phase is beneficial to corrosion resistance as the anodic corrosion currents decreased with increasing amount of ϵ phase.

5. Conclusion

The mechanical and corrosion properties of the duplex treated S154 (nitrided- CrN/NbN nano-scale multilayer PVD coating) was found to be excellent. Low-pressure pulse plasma nitriding process was used to produce pre-treatments for a PVD coating and the ABS process with Cr ion etching made it possible to establish a very good adhesion on all samples despite the compound layer at the surface of the samples. The composition of the compound layer was found to greatly affect the properties of the duplex treated samples. Based on the results of this study, a nitriding process that creates a hard surface layer would give the best wear properties for the duplex treated relatively soft and ductile steel such as S154. The hard PVD coating alone cannot protect the soft steels against wear as the insufficient load bearing capacity will cause quick failure of the coating as shown by the high wear coefficient of the CrN/NbN on untreated S154 steel. The good results can be achieved with a nitriding process where a hard compound layer is allowed to form on the surfaces. The composition of the compound layer can be tailored to the specific application by carefully controlling the nitriding process. In this study two phases γ' (Fe₄N) and ϵ (Fe₃N) were detected in the compound layer. Samples with ϵ phase rich compound layer were noted to have higher substrate surface hardness resulting in excellent sliding wear resistance in combination the CrN/NbN coating. For the best performing sample (Sample 1, 48% ϵ phase) the wear of the duplex treated S154 was similar to CrN/ NbN coated M2 HSS despite having only less than half of the substrate hardness. The duplex treatment also gave significant improvement to the corrosion resistance. The anodic corrosion currents of the duplex treated samples were up to 3 orders of magnitude lower than with samples with the same PVD coating.

The samples with ϵ phase rich compound layer had the highest the corrosion resistance. The ϵ phase hard phase is however subject to brittle fracture when subjected to deformation or impacts as demonstrated by scratch and impact test results. The sample with the compound

layer consisting mainly of the softer γ' phase could not match the wear and corrosion performance of the other samples, yet it had excellent adhesion and impact resistance. Also the thicker case depth and the compound layer can provide better support at high loads as demonstrated by the smallest impact crater.

References

- [1] W.-D. Münz, D.B. Lewis, P.Eh. Hovsepian, C. Schönjahn, A. Ehasarian, I.J. Smith, *Surf. Eng.* 17 (2001) 15.
- [2] B. Navinšek, P. Pajan, I. Milošev, *Surf. Coat. Technol.* 116-119 (1999) 476.
- [3] C. Schönjahn, L.A. Donohue, D.B. Lewis, W.-D. Münz, R.D. Twesten, I. Petrov, *J. Vac. Sci. Technol., A* 18 (4) (2000) 1718.
- [4] P.Eh. Hovsepian, D.B. Lewis, W.-D. Münz, *Surf. Coat. Technol.* 133-134 (2000) 166.
- [5] B. Podgornik, J. Vižintin, *Vacuum* 68 (2003) 39.
- [6] M. Zlatanović, D. Kakas, Lj. Maribrada, A. Kunosić, W.-D. Münz, *Surf. Coat. Technol.* 64 (1994) 173.
- [7] M. Fenker, M. Balzer, R.V. Büchi, H.A. Jehn, H. Kappl, J.-J. Lee, *Surf. Coat. Technol.* 163-164 (2003) 169.
- [8] P.Eh. Hovsepian, D.B. Lewis, W.-D. Münz, S.B. Lyon, M. Tomlinson, *Surf. Coat. Technol.* 120-121 (1999) 535.
- [9] M. Tomlinson, S.B. Lyon, P. Hovsepian, W.-D. Münz, *Vacuum* 53 (1999) 117.
- [10] J.M. O'Brien, D. Goodman, *ASM Metals Handbook*, vol 4, 1991, p. 420.
- [11] B. Podgornik, J. Vižintin, O. Wänstrand, M. Larsson, S. Hogmark, H. Ronkainen, K. Holmberg, *Wear* 249 (2001) 254.
- [12] A. Kagiya, K. Terakado, R. Urao, *Surf. Coat. Technol.* 169-170 (2003) 397.
- [13] P. Panjan, I. Urankar, B. Navinšek, M. Terčelj, R. Turk, M. Čekada, V. Leskovšek, *Surf. Coat. Technol.* 151-152 (2002) 505.
- [14] M. Pellizzari, A. Molinari, G. Straffelini, *Surf. Coat. Technol.* 142-144 (2001) 1109.
- [15] J.C.A. Batista, C. Godoy, G. Pintaúde, A. Sinatora, A. Matthews, *Surf. Coat. Technol.*, Article (in press).
- [16] J.-D. Kamminga, R. Hoy, G.C.A.M. Janssen, E. Lugscheider, M. Maes, *Surf. Coat. Technol.*, Article (in press).
- [17] G. Nayal, A.P. Ehasarian, K.M. Macak, R. New, W.-D. Münz, I.J. Smith, *E-MRS 2000 proceedings*, 2000.
- [18] P.Eh. Hovsepian, W.-D. Münz, *Society of Vacuum Coaters, 45th Annual Technical Conference Proceedings*, 2002.
- [19] C. Schönjahn, H. Paritong, W.-D. Münz, R.D. Twesten, I. Petrov, *J. Vac. Technol., A* 19 (4) (2001) 1392.
- [20] P.Eh. Hovsepian, D.B. Lewis, W.-D. Münz, A. Rouzaud, P. Juliet, *Surf. Coat. Technol.* 116-119 (1999) 727.

- [21] F.T. Hoffmann, P. Mayr, ASM handbook Vol. 18 Friction, Lubrication and Wear Technology, ASM International, 1991, p. 878.